Structural and conductivity studies of ammonium chloride doped agar–agar biopolymer electrolytes for electrochemical devices

S. Selvalakshmi[1],* iD , D. Vanitha[4], P. Saranya[5], S. Selvasekarapandian[3], T. Mathavan[2], and M. Premalatha[1,3]

[1] *Department of Physics, The Standard Fireworks Rajaratnam College for Women, Sivakasi, Tamil Nadu, India*

[2] *Department of Physics, N.M.S.S.V.N College, Nagamalai, Madurai, Tamil Nadu, India*

[3] *Materials Research Centre, Coimbatore, Tamil Nadu, India*

[4] *Department of Physics, Kalasalingam Academy of Research and Education, Krishnankoil, Tamil Nadu, India*

[5] *International Research Centre, Kalasalingam Academy of Research and Education, Krishnankoil, Tamil Nadu, India*

ABSTRACT

A new approach of solid polymer electrolyte (SPE) has been synthesized by agar doped with ammonium chloride and characterized by X-ray diffraction measurements, Fourier transform infrared spectroscopy and impedance spectroscopy. The highest ionic conductivity value of 4×10^{-3} S cm^{-1} has been achieved at room temperature for the SPE containing a concentration of 60 mol% agar with 40 mol% of NH$_4$Cl. The prepared biopolymer electrolytes exhibit Arrhenius behaviour and dielectric effects of the prepared samples are studied. Wagner's polarisation technique is used to find the ionic transference number, which is 0.99. Linear sweep voltammetry is used to investigate electrochemical stability. The best conductive film is used to build a battery and a fuel cell, with output voltages of 1.89 V and 541 mV, respectively.

1 Introduction

As of late, research on solid polymer electrolytes (SPEs) has acquired gigantic interest because of their application in super capacitors, electro chromic gadgets, energy units, solid-state batteries and sensors [1–5]. SPEs are reasonable for working at high-temperature and having great mechanical properties. Polymers like polyethene oxide (PEO) [6], polyvinyl alcohol (PVA) [7], biopolymers like methylcellulose [8] and chitosan [9] have been considered in the advancement of SPEs. However, no solid polymer electrolyte has arrived at maximum ionic conductivity at surrounding temperatures, other than Nafion.

Agar had been broadly used in food, pharmaceutical, micro-biological, medical and other industries. The use of agar in the field of electrochemistry has also been investigated [10, 11]. As a natural biopolymer, agar is more interesting than the synthetic polymers as an electrolyte in different fields

owing to its higher biocompatibility and biodegradability, which make it more environmental-friendly.

In order to accomplish a significant ionic conductivity, bio-viable and bio-degradable SPE, a novel biopolymer electrolyte with a blend of agar–agar and NH_4Cl have been prepared and characterized in the current review. Among the sustainable biopolymers, agar is striking because they are galactose-rooted polysaccharides extricated from seaweed having the comparable chemical structure of rehashing unit of disaccharide. A miscellaneous combination of polysaccharides: agaropectin and agarose is called agar. The two polymers share a similar galactose-supported backbone, agaropectin is intensely changed with the acidic side-groups, like sulphate and pyruvate; charge of the agarose was neutral. Agar–agar is a direct polysaccharide comprised of rotating β-(1,3)- and α-(1,4)-connected galactose deposits [12]. The appropriateness of agar gel is an option for riveted solid polymer electrolyte and Kasem has accounted for it as a polymer electrolyte for electrochemical experiments [13]. Leones et al. [14] has found a conductivity value of 2.35×10^{-5} S cm^{-1} for agar-based polymer electrolyte with 1-ethyl-3-methylimidazolium acetic acid derivation structure at surrounding temperature. Ionic conductivity worth 1.1×10^{-4} S cm^{-1} at room temperature has been accounted for by Ellen Raphael et al. [15] for agar with acetic acid. Among the inorganic salts, ammonium salts have been accounted for as great proton givers. Ammonium-based salt is picked for this new approach since proton-conducting electrolytes have been perceived for their appropriateness in the utilization of low-energy density gadgets [16, 17]. Vijaya et al. [18] has announced a conductivity of 4.52×10^{-4} S cm^{-1} for biopolymer electrolyte dependent on Pectin doped with NH_4Cl. Sikkanthar et al. [19] has portrayed a polymer electrolyte dependent on PAN with NH_4Cl which displayed an ionic conductivity in the range 10^{-3} S cm^{-1}. In view of these reports, biopolymer electrolyte with another blend of agar and NH_4Cl has been prepared and characterised in the current review to accomplish high ionic conductivity.

2 Experimental details

2.1 Electrolyte preparation

Agar–agar of average molecular weight 120,000 (Condo-Forja, Madrid) and NH_4Cl (spectrum) were taken for this work. By the Solution-Casting technique, different compositions of agar and NH_4Cl were doped to form membranes. The mixture was magnetically stirred and poured in petri dishes. The samples were dehydrated by the hot air oven. Solvent free SPE films were collected after 48 h.

2.2 Electrolyte characterization

The membranes were studied by X-ray diffraction analysis (XRD) using Cu Kα radiation at room temperature on a Philips X' Pert PRO diffractometer. The molecular interaction and chemical composition of the membranes were analysed from the FTIR spectra obtained from SHIMADZU-IR Affinity-1 Spectrometer in the extend of 400–4000 cm^{-1}. Impedance spectra of the prepared membranes were obtained using HIOKI 3532 LCZ meter in the frequency extend 42 Hz–1 MHz, over the temperature range 303–343 K. For determining the transference number, Wagner's DC polarization method was employed. The electrochemical stability of the polymer membrane was decided by linear sweep voltammetry using 0.1 mV s^{-1} scan rate. Formation of fuel cell and solid state electrochemical cell were done by using the best conducting polymer electrolyte.

3 Results and discussions

3.1 X-ray diffraction analysis

To examine the nature of agar-based films and X-ray diffraction patterns of the SPE with various compositions of NH_4Cl are contemplated and are displayed in Fig. 1.

The diffractograms (Fig. 1) of agar–NH_4Cl show expansive dispersed bands at the range of $2\theta = 20°$, $30°$ with a shoulder top at $2\theta = 13°$ which have effectively been accounted by Raphael et al. [15]. It is observed that the relative intensities of these peaks decline with the expansion of NH_4Cl. The broadness of the peaks increment with the increment of NH_4Cl. The reduction in intensity and expansion in the width
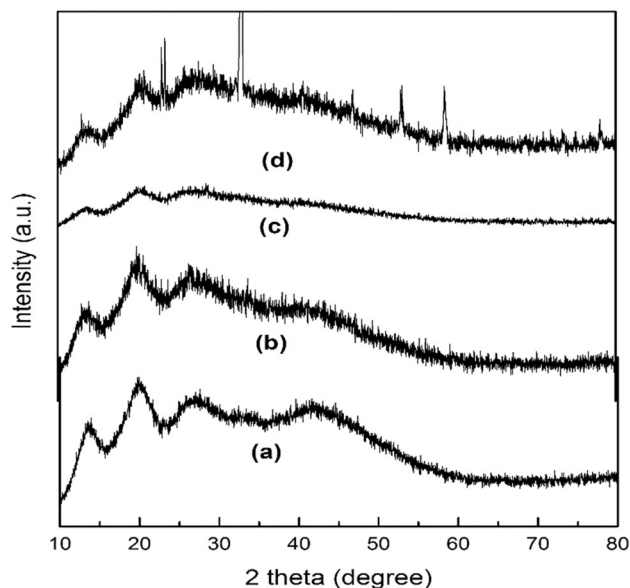
Fig. 1 XRD patterns of **a** pure agar and agar doped with **b** 30 mol% NH$_4$Cl **c** 40 mol% NH$_4$Cl **d** 50 mol% NH$_4$Cl

Fig. 2 FTIR spectra of **a** pure agar and agar doped with **b** 30 mol% NH$_4$Cl **c** 40 mol% NH$_4$Cl **d** 50 mol% NH$_4$Cl

of the XRD peaks uncover that the amorphous nature of the agar–agar increments because of the addition of the dopant. It is clear from the figure that the composition of 60 mol% agar with 40 mol% NH$_4$Cl is more amorphous. The sharp peaks at $2\theta = 23°$, $32.82°$, $47°$, $53°$ (JCPDS document no. 34-0710) in 50 mol% agar with 50 mol% NH$_4$Cl are credited to NH$_4$Cl because of the appearance of undissociated salt in the polymer lattice.

3.2 Fourier transforms infrared analysis

FTIR is a promising strategy to track down the idea of functional groups and furthermore the development of any new bonds due to doping in the SPE framework. Figure 2 shows the FTIR spectra of pure agar SPE film and agar doped with NH$_4$Cl in various molar proportions.

From Table 1, the absorption peaks for pure agar and different pieces of agar doped with NH$_4$Cl SPE films are shown. The wideband at 3404 cm^{-1} relates to the stretching of the functional compound O–H hydroxyl gathering of agar that takes part in entomb and intra-atomic hydrogen bond arrangement and has been moved slightly for all the compositions [20]. A trademark peak of the pure sample is at 934 cm^{-1} which is related to the in salt doped agar 3,6-anhydro galactose bridges with a minor shift [21]. The absorption band at 1370 cm^{-1} is because of the
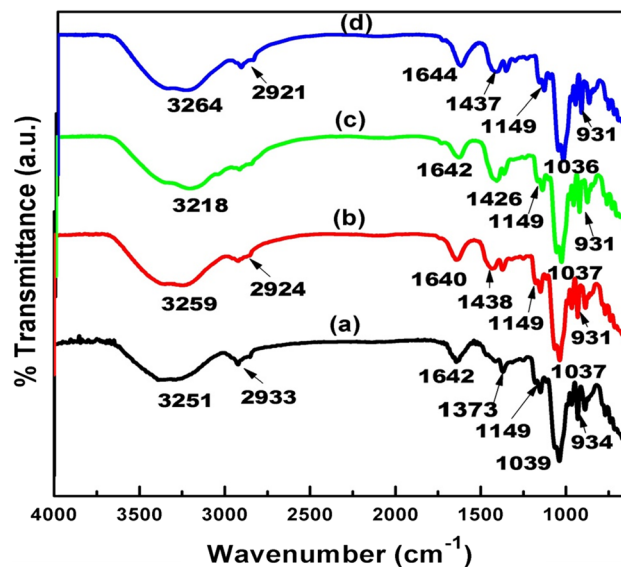
vibration mode of sulphate groups and it is viewed as moved to higher wavenumbers [22] in the agar doped with NH$_4$Cl samples. The absorption peak at 1149 cm^{-1} is because of the vibration mode of ester-sulphate connect vibrations. The extreme pinnacle saw at 1038 cm^{-1} is nearly found in all polysaccharides. It is predominantly because of the coupling of the C–C or the C–O extending modes with the bending modes of C–O–H [23, 24].

The NH$_4$Cl salt splits into two ions: NH^{4+} and Cl$^-$. The NH^{4+} ions are made up of two identically bound hydrogen atoms, a third hydrogen atom bound more tightly, and a fourth hydrogen atom bound more weakly. The polar group of the agar polymer matrix interacts with the poorly bound H$^+$ of NH$_4$, which is easily dissolved by the effect of an electric field [25]. The connection between the salt with the biopolymer matrix can cause the bands to shift and the intensity of the bands to alter. The aforesaid finding supports the creation of a complex between the polymer and the salt.

3.3 AC impedance spectroscopic analysis

AC Impedance measurements are utilized to calculate ionic conductivity of the electrolyte. Figure 3a displays the Cole Cole plots of agar/NH$_4$Cl SPE films with diverse concentrations of NH$_4$Cl at 303 K. The plot of pure agar and 90 mol% agar:10 mol% NH$_4$Cl comprise of a high-frequency semicircle and a spike

Table 1 Transmittance peaks for agar and different compositions of agar doped with NH₄Cl SPE films

Wavenumber (cm^{-1})				Assignment
Pure agar	70% agar:30% NH$_4$Cl	60% agar:40% NH$_4$Cl	50% agar:50% NH$_4$Cl	
3404	3259	3218	3264	O–H stretching
2933	2924	–	2921	CH$_2$ stretching
1642	1640	1642	1644	C=O stretching
–	1438	1426	1437	C–O–H bending
1373	1370	1382	1370	CH$_2$ bending
1149	1149	1148	1149	Ester-sulphate link vibrations
1039	1037	1037	1036	CH$_2$ scissoring
934	931	931	931	Ester sulphate link vibration

at low-frequency. The high-frequency semicircle may possibly be the bulk properties of the polymer electrolyte [26]. In the Impedance Spectroscopic analysis, bulk resistance is measured from the Cole–Cole plot [27]. The applied field polarises the stationary polymer chains and the dominance of electrode polarisation is responsible for the low frequency spike.

For other compositions, the plots show only the inclined spike suggesting that the samples are purely resistive.

Conductivity of the SPE films can be calculated from Eq. (1)

$$\sigma = l/(R_b \times A) \text{ S cm}^{-1}. \tag{1}$$

In the above equation, 'l' is film thickness, 'A' is called area between electrolyte and electrode and 'R_b' is denoted as a bulk resistance. The bulk resistance R_b of the SPE is attained from the end of the semicircle and the straight line inclined with the Z'-axis.

It is perceived that the 60 mol% agar:40 mol% NH₄Cl composition gives high conductivity of 4×10^{-3} S cm^{-1}. The rise in conductivity may possibly be due to large amount mobile ion concentration. The decrease in conductivity of SPE films with high salt concentration (50 mol% agar:50 mol% NH₄Cl) may be due the formation of ion clusters which is evidenced from the XRD pattern. Table 2 displays, ionic conductivity of different combinations of agar with NH₄Cl at various temperatures. It is seen that ionic conductivity increments with expansion in temperature. Polymer chain fragments would be enhanced at higher temperatures, resulting in an increase in absolute ionic conductivity.

Figure 3b shows the variation of real part of impedance (Z') with frequency for the highest conductivity membrane (60 mol% agar:40 mol% NH₄Cl) at different temperatures.

3.4 Conductance spectra analysis

From Fig. 4, at room temperature, the frequency relation with conductivity for various mixes of agar and NH₄Cl polymer electrolytes are shown. The two regions of the plots are: a low frequency dispersion zone caused by space charge polarisation at the obstructive electrodes and a frequency independency of plateau region, which match with dc conductivity. By inferring from the plateau region to zero frequency, the dc conductivity value can be determined.

The σ$_{dc}$ values specify a rise in conductivity with increase in frequency and it stay almost steady from definite frequency. The highest dc conductivity is observed for 60 mol% agar:40 mol% NH₄Cl polymer membrane. It is also observed that dc conductivity is enhanced with the high salt concentration up to 40 mol% which is ascribed to the large number of mobile charge carriers and all ions contribute to the charge transport in the presence of external electric field. The decrease in conductivity for the agar membrane with 50 mol% of NH₄Cl may be attributed to the presence of ion. Figure 5 shows the conduction spectra for the good conductivity membrane of composition 60 mol% agar:40 mol% NH₄Cl at different temperatures. There are two regions in the spectra. The low frequency dispersive region and higher frequency plateau region which corresponds to DC conductivity of material. The extrapolation of plateau regions gives the value of DC conductivity. The frequency independent plateau region shifted towards the lower frequency dispersion region and the plateau region increased while increasing the salt
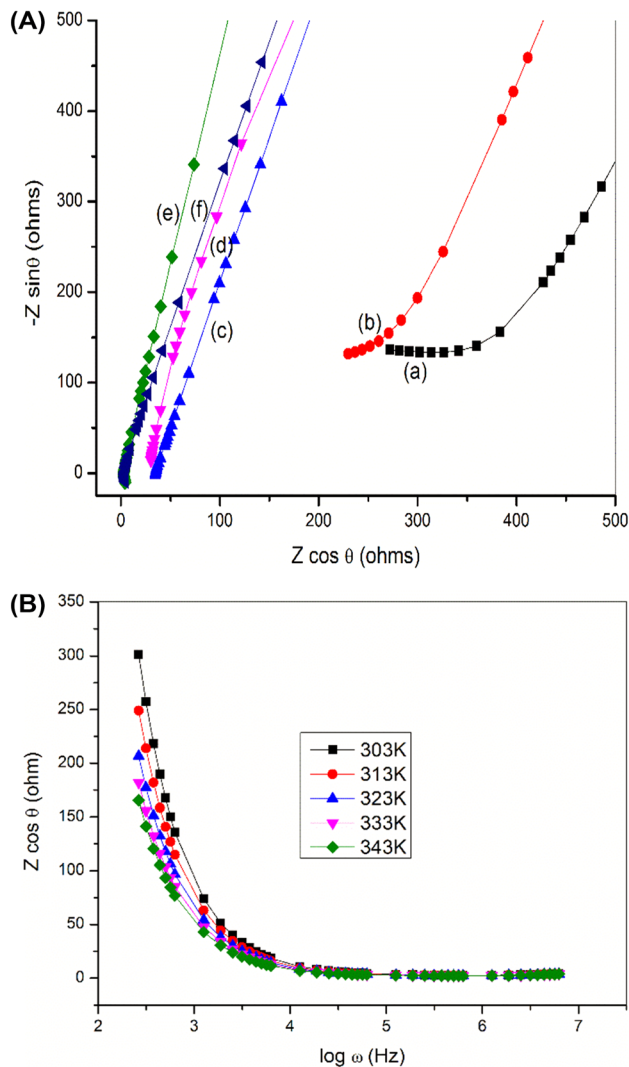
Fig. 3 a Cole–cole plot for various compositions of agar with NH$_4$Cl at 303 K. **a** Pure agar **b** 90 mol% agar:10 mol% NH$_4$Cl **c** 80 mol% agar:20 mol% NH$_4$Cl **d** 70 mol% agar:30 mol% NH$_4$Cl **e** 60 mol% agar:40 mol% NH$_4$Cl **f** 50 mol% agar:50 mol% NH$_4$Cl. **b** Variation of real part of impedance with frequency at different temperatures for 60 mol% agar:40 mol% NH$_4$Cl polymer membrane

concentration [28]. This is due to the enhancement of the available free charge carriers in the system. The rise in conductivity depends on the temperature owing to the reduction in the viscosity of the solution [29].

3.5 Temperature dependent conductivity

The conductivity for all SPE films depends on temperature which is shown in Fig. 6.

The Arrhenius equation for comparing experimental data,

$$\sigma T = \sigma_{\mathrm{o}} \exp(-E_{\mathrm{a}}/kT), \tag{2}$$

where "σ"$_{\mathrm{o}}$ denotes the pre-exponential factor, "E_{a}" denotes the activation energy, and "k" denotes the Boltzmann constant. The linear fit is revealed to be close to unity, for regression values. This shows that the prepared biopolymer membranes obey the temperature-dependent ionic conductivity and fulfils the Arrhenius relationship.

When the temperature rises, a sector's vibrational energy is sufficient to provide impetus against the force operated by its nearby atoms, resulting in a little area of space enclosing its own volume in which vibrational motion can arise. As a result, the mobility of the polymer segments increases, allowing ions to float freely along the polymer chain, thereby increases the conductivity.

Table 3 shows the activation energy obtained from log (σ) vs $1000/T$ graphs. The sample with the highest conductivity, 60 mol% agar:40 mol% NH$_4$Cl, has the lowest activation energy of 0.04 eV.

3.6 Compositional dependence of conductivity

Figure 7 shows the conductivity and the activation energy as a function of different concentration of NH$_4$Cl at room temperature.

As the conductivity of the sample increases, Ea drops, meaning that ions in highly conducting samples require less energy to migrate.

3.7 Transference number measurement

The polymer electrolytes which are responsible for the conduction have been investigated using the technique called Wagner's dc polarisation [30]. The fluctuation in polarisation current as the function of time is depicted in Fig. 8. The transference number is determined using

$$t_{\mathrm{ion}} = 1 - -I_{\mathrm{f}}/I_{\mathrm{i}}, \tag{3}$$

$$t_{\mathrm{ele}} = 1 - t_{\mathrm{ion}}, \tag{4}$$

where 'I_{i}' and 'I_{f}' are the initial and final currents, respectively.

When a dc potential (1.08 V) is applied between the two aluminium electrodes sandwiching the best

Table 2 Ionic conductivity of the various compositions of agar with NH$_4$Cl at different temperatures

| Composition of agar:NH$_4$Cl	Ionic conductivity (σ) (S cm^{-1}) for different compositions of agar:NH$_4$Cl				
	303 K	313 K	323 K	333 K	343 K
Pure agar–agar	$2.38 \pm 0.02 \times 10^{-5}$	$2.58 \pm 0.02 \times 10^{-5}$	$3.91 \pm 0.01 \times 10^{-5}$	$6.60 \pm 0.03 \times 10^{-5}$	$6.84 \pm 0.01 \times 10^{-5}$
90:10	$4.45 \pm 0.01 \times 10^{-5}$	$5.39 \pm 0.01 \times 10^{-5}$	$6.12 \pm 0.02 \times 10^{-5}$	$6.56 \pm 0.01 \times 10^{-5}$	$9.00 \pm 0.02 \times 10^{-5}$
80.20	$4.78 \pm 0.1 \times 10^{-5}$	$7.76 \pm 0.03 \times 10^{-5}$	$1.74 \pm 0.01 \times 10^{-4}$	$2.47 \pm 0.02 \times 10^{-4}$	$3.28 \pm 0.01 \times 10^{-4}$
70:30	$9.85 \pm 0.01 \times 10^{-5}$	$1.35 \pm 0.04 \times 10^{-4}$	$2.64 \pm 0.03 \times 10^{-4}$	$5.06 \pm 0.03 \times 10^{-4}$	$5.98 \pm 0.01 \times 10^{-4}$
60:40	$4 \pm 0.02 \times 10^{-3}$	$4.15 \pm 0.1 \times 10^{-3}$	$4.37 \pm 0.02 \times 10^{-3}$	$4.68 \pm 0.03 \times 10^{-3}$	$4.79 \pm 0.1 \times 10^{-3}$
50:50	$8.79 \pm 0.02 \times 10^{-4}$	$1.14 \pm 0.02 \times 10^{-3}$	$1.33 \pm 0.03 \times 10^{-3}$	$1.46 \pm 0.01 \times 10^{-3}$	$1.55 \pm 0.01 \times 10^{-3}$
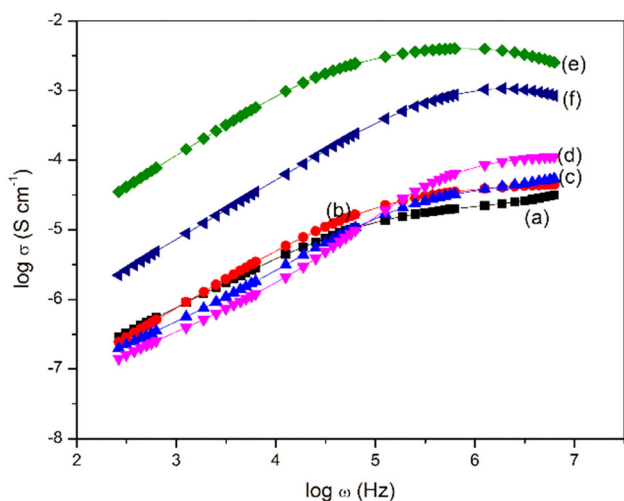
Fig. 4 Frequency dependent conductivity plot for various compositions of agar with NH$_4$Cl at 303 K
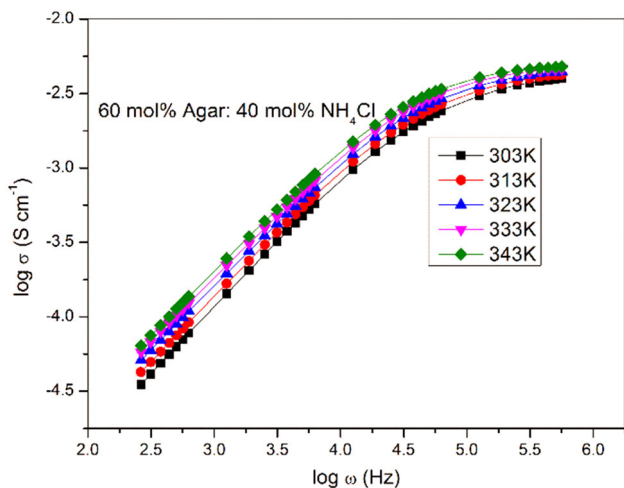

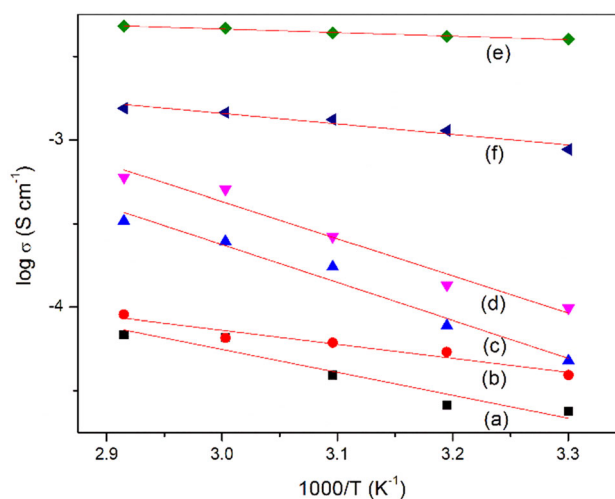**Fig. 5** Frequency dependent conductivity plot for 60 mol% agar with 40 mol% NH$_4$Cl at various temperatures

Fig. 6 Temperature dependent conductivity graph for various compositions of agar with NH$_4$Cl **a** pure agar **b** 90 mol% agar:10 mol% NH$_4$Cl **c** 80 mol% agar:20 mol% NH$_4$Cl **d** 70 mol% agar:30 mol% NH$_4$Cl **e** 60 mol% agar:40 mol% NH$_4$Cl **f** 50 mol% agar:50 mol% NH$_4$Cl

conductivity biopolymer electrolyte (60 mol% agar:40 mol% NH$_4$Cl), the polarisation current is measured by the variation in time.

The total ionic transference number of 0.99 is obtained for the sample with best conductivity is 60 mol% agar:40 mol% the concentration of NH$_4$Cl. The ionic transference number has a value near to unity. So that, the ions play a major role in charge transport in this polymer electrolyte.

3.8 Transport parameters

Using the equations below, the diffusion coefficients of anions and cations of polymer electrolyte are obtained [31].

Table 3 Activation energy values of agar:NH$_4$Cl polymer electrolytes

Composition of agar:NH$_4$Cl	Regression value	Activation energy (eV)
Pure	0.991	0.40
90:10	0.966	0.25
80:20	0.961	0.24
70:30	0.928	0.16
60:40	0.975	0.04
50:50	0.923	0.13
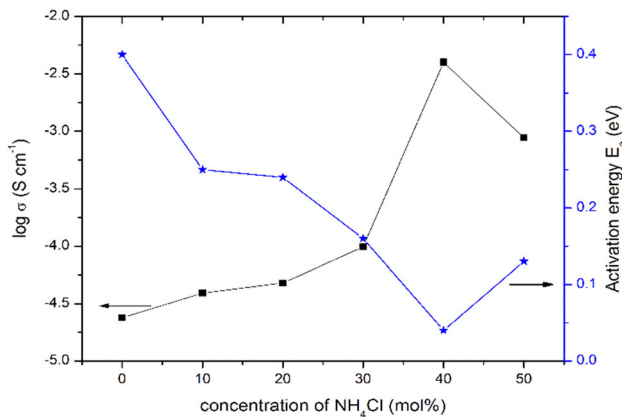
Fig. 7 Variation of conductivity and activation energy of agar:NH$_4$Cl as a function of salt concentration
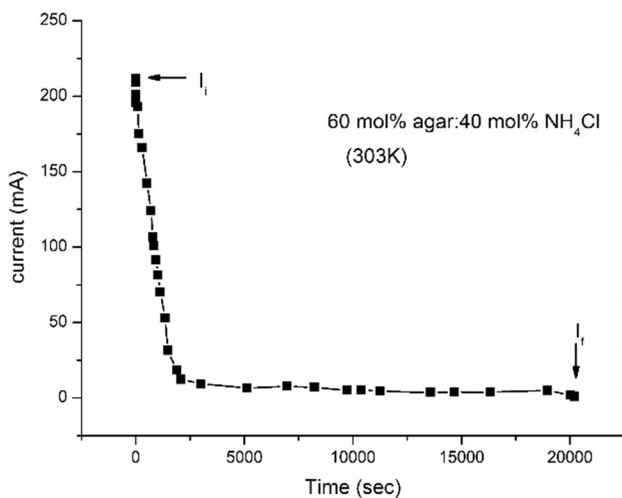
Fig. 8 Polarisation current vs. time plot of 60 mol% agar + 40 mol% NH$_4$Cl

$$n = N\rho$$
$$\times \text{ molar ratio of salt/molecular weight of the salt}$$

$$D_+ = D \times t_+,$$

$$D = D_+ + D_- = kT\sigma/ne^2.$$

The ionic mobility of all the samples have been determined using the equation

$$\mu_+ = \mu t_+,$$
$$\mu = \mu_+ + \mu_- = \sigma/ne,$$

where ρ is density of the salt, N is the Avagadro number, e charge of the electron, k is the Boltzmann constant, T is the absolute temperature, n is the number of charge carriers, μ_-, μ_+ is the ionic mobility of anion and cation respectively, D_-, D_+ is the diffusion coefficient of anion and cation respectively.

The diffusion coefficient and ionic mobility of cations and anions calculated for all compositions of polymer membrane are shown in Table 4. The value of both diffusion coefficient (D) and mobility (μ) are increased up to the sample 60 mol% agar:40 mol% NH$_4$Cl. The cation value of D and μ is higher value than anion in all the polymer blend electrolytes. From this, it is concluded that D and μ are responsible for the enhancement of ion conductivity in 60 mol% agar:40 mol% NH$_4$Cl polymer blend electrolytes [32].

3.9 Dielectric spectra analysis

The complex permittivity $\varepsilon^* = \varepsilon' - i\varepsilon''$, is commonly used to describe the dielectric response, with the real ε' component which is attributed to charge accumulation and the imaginary ε'' component ascribes to energy loss in every cycle of the applied electric field. At 303 K, the variation in ε' and ε'' with different compositions for agar with NH$_4$Cl polymer electrolytes is shown in Fig. 9a, b. ε' and ε'' have very high values at low frequencies and are rather stable at higher frequencies [33]. Energy absorption or attenuation can explain the variability of ε'' with frequency. The intermittent setback of the electric field at higher frequencies is in some way that there is no surplus ion diffusion in the field direction, causing a reduction in dielectric constant. [34].

The graph of the frequency dependence of ε'' of (60 mol% agar:40 mol% NH$_4$Cl) at room temperature

Table 4 Transport parameters for all compositions of agar:NH$_4$Cl

| Compositions	n (cm^{-3})	D (cm^2 s^{-1})	D_+ (cm^2 s^{-1})	D_- (cm^2 s^{-1})	μ (cm^2 v^{-1} s^{-1})	μ_+ (cm^2 v^{-1} s^{-1})	μ_- (cm^2 v^{-1} s^{-1})
90:10	3.284×10^{20}	2.213×10^{-8}	2.051×10^{-8}	1.620×10^{-9}	8.469×10^{-7}	7.850×10^{-7}	6.181×10^{-8}
80:20	7.189×10^{20}	2.799×10^{-8}	2.642×10^{-8}	1.560×10^{-10}	1.071×10^{-6}	1.011×10^{-6}	6.000×10^{-8}
70:30	1.198×10^{21}	6.898×10^{-8}	6.643×10^{-8}	2.544×10^{-9}	2.639×10^{-6}	2.542×10^{-6}	9.685×10^{-8}
60:40	1.793×10^{21}	3.649×10^{-7}	3.631×10^{-7}	1.728×10^{-9}	1.394×10^{-5}	1.387×10^{-5}	6.660×10^{-8}
50:50	2.545×10^{21}	5.641×10^{-8}	5.291×10^{-8}	3.494×10^{-9}	2.158×10^{-6}	2.024×10^{-6}	1.331×10^{-7}
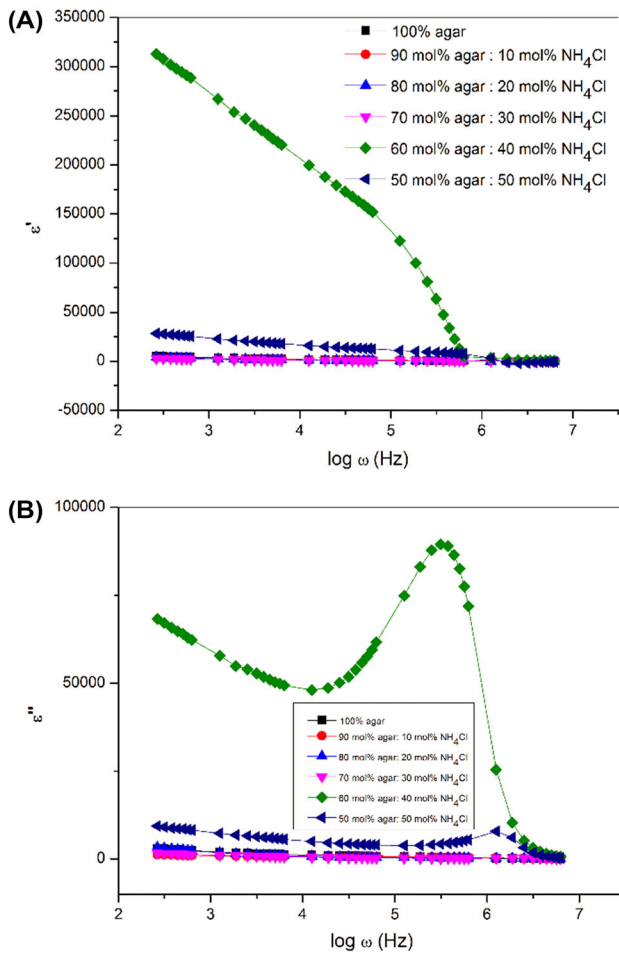
Fig. 9 a Frequency response of dielectric constant of various compositions **a** 100% agar **b** 90 mol% agar:10 mol% NH$_4$Cl **c** 80 mol% agar:20 mol% NH$_4$Cl **d** 70 mol% agar:30 mol% NH$_4$Cl **e** 60 mol% agar:40 mol% NH$_4$Cl **f** 50 mol% agar:50 mol% NH$_4$Cl. **b** Frequency response of dielectric loss of various compositions **a** 100% agar **b** 90 mol% agar:10 mol% NH$_4$Cl **c** 80 mol% agar:20 mol% NH$_4$Cl **d** 70 mol% agar:30 mol% NH$_4$Cl **e** 60 mol% agar:40 mol% NH$_4$Cl **f** 50 mol% agar:50 mol% NH$_4$Cl

shows a large frequency relaxation peak that could be done by side group dipole movement [35, 36].

3.10 Linear sweep voltammetry

The electrochemical stability is the major parameter to estimate the polymer electrolyte's stability. The maximum conducting polymer electrolyte (60% agar:40% NH$_4$Cl) is developed to determine the polymer electrolyte's capacity to tolerate the operating voltage of a battery system in the electrochemical stability window of. A linear sweep voltammetry is using an inert stainless steel as the working electrode and the stainless steel plates as the reference and the counter electrodes. The stainless steel/60% agar:40% NH$_4$Cl polymer electrolyte cell is built and used at a 1 mV s^{-1} scan rate from 0 to 5 V. The linear sweep voltammogram of the best conducting polymer electrolyte (60% agar:40% NH$_4$Cl) as a function of voltage is shown in Fig. 10.

The breakdown voltage can be determined by the extrapolation of the straight line from the LSV curves
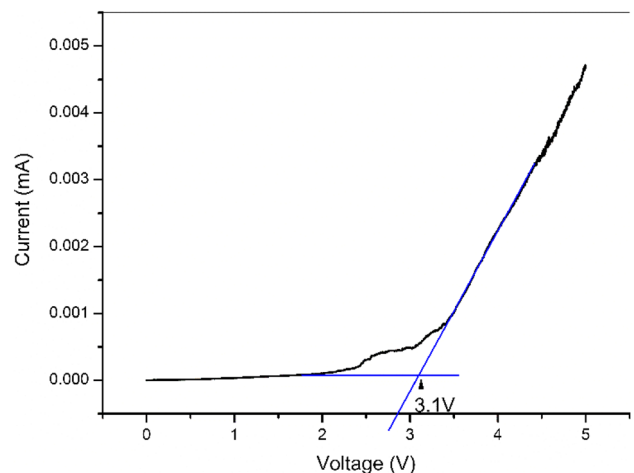

Fig. 10 Linear sweep voltammogram for the highest conducting polymer electrolyte film of 60% agar:40% NH$_4$Cl
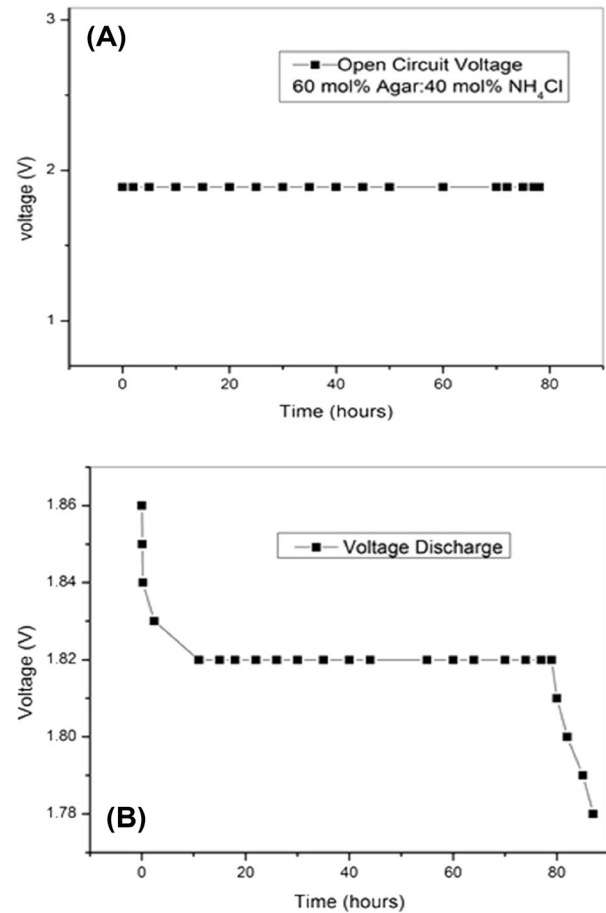
Fig. 11 **a** Open circuit voltage vs time for the cell. **b** Discharge characteristics for the cell

Table 5 Cell parameters calculated for plateau region for the discharge curve

S. no	Cell parameters	Agar 60%:NH$_4$Cl 40%
1	Open circuit voltage (OCV)	1.89 V
2	Weight of cathode material	1.027 mg
3	Weight of anode material	0.467 mg
4	Weight of the cell	1.576 mg
5	Thickness of anode	2.214 mm
6	Thickness of cathode	2.242 mm
7	Area of the cell	1.1304 cm^2
8	Discharge time	78 h

[37]. The electrochemical stability window for the 60% agar–40% NH$_4$Cl system is up to 3.1 V, according to the linear sweep voltammogram. As a result, this polymer electrolyte is well-suited for use in proton batteries with a working voltage of 3.1 V.
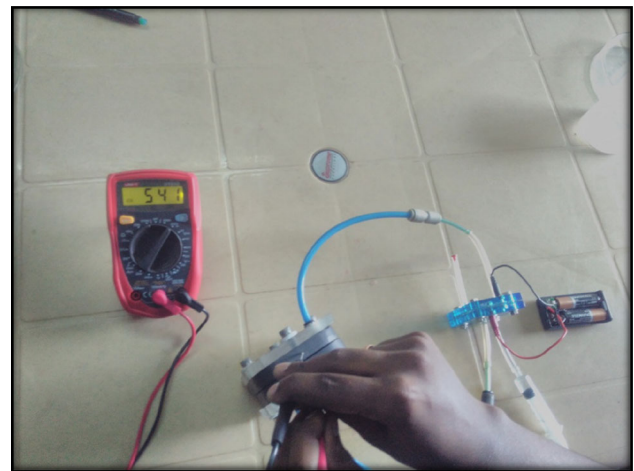

Fig. 12 PEM fuel cell with 60 mol% agar:40 mol% NH$_4$Cl polymer membrane

3.11 Battery characterization

In a solid state battery, the highest conductivity polymer film (60 mol% agar:40 mol% NH$_4$Cl) is

sandwiched between two electrodes. The cathode material in this study is composed of lead oxide (PbO_2), graphite, vanadium pentaoxide (V_2O_5),and a 60 mol% agar:40 mol% NH_4Cl SPE film in the ratio of 8:2:1:0.5. Zinc powder, zinc sulphate, and graphite are used to make the anode in a 3:1:1 ratio. Thin pellets serve as the cathode and anode, respectively. The highest conductivity sample is sandwiched between the anode and prepared cathode, placed in the battery holder, which is connected with the multimeter for determining the open circuit voltage (OCV).The variation of open circuit voltage with time is shown in Fig. 11a and the charge discharge characteristics of the prepared electrochemical cell, is shown Fig. 11b. Table 5 gives the cell parameters of the prepared cell.

3.12 Construction of single PEM fuel cell

The PEM fuel cell used in this work is made up of bipolar graphite plates encased in silicon gaskets and carved with a 7.4 cm^2 parallel flow channel. Two acrylic foundation plates hold these plates in place. Platinized carbon cloths with an area of 8.4 cm^2 are placed above the flow channels of the either graphite plates, that act as cathode and anode, with the platinum layer acting as a catalyst. Between the electrodes, best proton conducting membrane (60 mol% agar:40 mol% NH_4Cl) is sandwiched. The fuels for the single PEM fuel cell are produced by applying a 3 V voltage to a tiny electrolyser, which produces hydrogen and oxygen.

The freshly fabricated PEM fuel cell with 60 mol% agar:40 mol% NH_4Cl biopolymer polymer electrolyte displayed a voltage of 541 mV and is presented in Fig. 12. The obtained voltage suggests that the biopolymer membrane with a mixture of agar and NH_4Cl is a worthy contender for battery and fuel cell applications.

4 Conclusion

Novel biopolymer membrane along with agar–agar and different compositions NH_4Cl is prepared by solution casting characterized by different techniques. Pattern of the XRD for agar + NH_4Cl displayed the decrease in the intensity of peaks confirms the decrease in crystallinity with the rise of salt concentration. FTIR investigations confirm the

complexation of NH_4Cl with the agar polymer. The conductivity is increased with dopant concentration and the maximum conductivity of 4×10^{-3} is reported for 60 mol% agar:40 mol% NH_4Cl. The ionic transport number measurements in the (agar:NH_4Cl) polymer electrolyte suggests that ions rather than electrons are responsible for the conduction. The dielectric constant and dielectric loss are higher for the 60 mol% agar:40 mol% NH_4Cl membrane, according to the dielectric analysis. The electrochemical stability window for the 60% agar–40% NH_4Cl system is up to 3.1 V, according to the linear sweep voltammogram. A higher conducting film is used to create an electrochemical cell with a voltage of 1.89 V as an open circuit voltage and the parameters of the cells are reported. Similarly, single PEM fuel cell is fabricated with 60 mol% agar:40 mol% NH_4Cl biopolymer electrolyte which exhibits a voltage of 541 mV.

Author contributions

All authors contributed to the study conception and design. Material preparation, data collection and analysis were performed by SS. The first draft of the manuscript was written by DV and all authors commented on previous versions of the manuscript. All authors read and approved the final manuscript.

Data availability

The datasets generated during and/or analysed during the current study are available from the corresponding author on reasonable request.

Declarations

Conflict of interest On behalf of all authors, the corresponding author states that there is no conflict of interest. The first author, Dr. SLI has received the technical support from The Standard Fireworks Rajaratnam College for Women.

References

1. Y.N. Sudhakar, M. Selvakumar, D.K. Bhat, Ionics (Kiel). **19**, 277 (2013)

2. A.K. Arof, N.E.A. Shuhaimi, N.A. Alias, M.Z. Kufian, S.R. Majid, J. Solid State Electrochem. **14**, 2145 (2010)

3. R.C. Agrawal, S.A. Hashmi, G.P. Pandey, Ionics (Kiel). **13**, 295 (2007)

4. E. Siebert, S. Rosini, R. Bouchet, G. Vitter, Ionics (Kiel). **9**, 168 (2003)

5. K.P. Singh, R.P. Singh, P.N. Gupta, Solid State Ionics **78**, 223 (1995)

6. L. Ismail, S.R. Majid, A.K. Arof, Mater. Res. Innov. **13**, 282 (2009)

7. I.S. Noor, S.R. Majid, A.K. Arof, Electrochim. Acta **102**, 149 (2013)

8. N.E.A. Shuhaimi, S.R. Majid, A.K. Arof, Mater. Res. Innov. **13**, 239 (2009)

9. S.R. Majid, A.K. Arof, Phys. B Condens. Matter **390**, 209 (2007)

10. L. An, T.S. Zhao, L. Zeng, Appl. Energy **109**, 67–71 (2013)

11. S.Y. Liew, J.C. Juan, C.W. Lai et al., Ionics **25**, 1291–1301 (2019)

12. A.M. Stephen, G.O. Phillips, P.A. Williams, *Food Polysaccharides and Their Applications* (CRC Press, Boca Raton, 2016)

13. K.K. Kasem, J. New Mater. Electrochem. Syst. **8**, 189–195 (2005)

14. M.M.S.R. Leones, F. Sentanin, L.C. Rodrigues, I.M. Marrucho, J.M.S.S. Esperança, A. Pawlicka, Syria Stud. **7**, 37 (2015)

15. E. Raphael, C.O. Avellaneda, B. Manzolli, A. Pawlicka, Electrochim. Acta **55**, 1455 (2010)

16. H. Nakajima, I. Honma, Solid State Ionics **148**, 607 (2002)

17. R. Pratap, B. Singh, S. Chandra, J. Power Sources **161**, 702 (2006)

18. N. Vijaya, S. Selvasekarapandian, G. Hirankumar, S. Karthikeyan, H. Nithya, C.S. Ramya, M. Prabu, Ionics (Kiel). **18**, 91 (2012)

19. S. Sikkanthar, S. Karthikeyan, S. Selvasekarapandian, D. Arunkumar, H. Nithya, K. Junichi, Ionics (Kiel). **22**, 1085 (2016)

20. J. Coates, Encycl. Anal. Chem. 10815 (2006).

21. J. Orduña-Rojas, D. Robledo, Bot. Mar. **45**, 459 (2002)

22. P. Guerrero, A. Etxabide, I. Leceta, M. Peñalba, K. De La Caba, Carbohydr. Polym. **99**, 491 (2014)

23. M.F.Z. Kadir, Z. Aspanut, S.R. Majid, A.K. Arof, Spectrochim. Acta Part A Mol. Biomol. Spectrosc. **78**, 1068 (2011)

24. M.H. Buraidah, L.P. Teo, S.R. Majid, A.K. Arof, Phys. B Condens. Matter **404**, 1373 (2009)

25. M. Hema, S. Selvasekerapandian, A. Sakunthala, D. Arunkumar, H. Nithya, Phys. B Condens. Matter **403**, 2740 (2008)

26. S.A. Hashmi, A. Kumar, K.K. Maurya, S. Chandra, J. Phys. D. Appl. Phys. **23**, 1307 (1990)

27. D. Vanitha, S.A. Bahadur, N. Nallamuthu, S. Athimoolam, A. Manikandan, J. Inorg. Organomet. Polym. Mater. **27**, 257 (2017)

28. R. Sehrawat, A. Sil, Ionics (Kiel). **21**, 673 (2015)

29. S. Das, A. Ghosh, Electrochim. Acta **171**, 59 (2015)

30. S. Ramesh, A.H. Yahaya, A.K. Arof, Solid State Ionics **152–153**, 291 (2002)

31. J.B. Wagner, C. Wagner, J. Chem. Phys. **26**, 1597 (1957)

32. O.E. Geiculescu, R. Rajagopal, S.E. Creager, D.D. DesMarteau, X. Zhang, P. Fedkiw, J. Phys. Chem. B **110**, 23130 (2006)

33. M.A. Jothi, D. Vanitha, S.A. Bahadur, N. Nallamuthu, Ionics (Kiel). **27**, 225 (2021)

34. C.S. Ramya, S. Selvasekarapandian, G. Hirankumar, T. Savitha, P.C. Angelo, J. Non. Cryst. Solids **354**, 1494 (2008)

35. K. Adachi, O. Urakawa, J. Non. Cryst. Solids **307–310**, 667 (2002)

36. S. Monisha, T. Mathavan, S. Selvasekarapandian, A. MiltonFranklinBenial, G. Aristatil, N. Mani, M. Premalatha, D. Vinothpandi, Carbohydr. Polym. **157**, 38 (2017)

37. J.C.H. Koh, Z.A. Ahmad, A.A. Mohamad, Ionics (Kiel). **18**, 359 (2012)